STRUCTURAL ANALYSIS OF A MICROSATELLITE LAUNCHER VEHICLE SUBMITTED TO EXTERNAL PRESSURE

Robert R. A. Oliveira[1], Giovani L. Zabot[2], Maikson L. P. Tonatto[1]

[1]Materials and Structures Mechanics Group (GMEC), Federal University of Santa Maria (UFSM)
3013, Taufik Germano Rd., Passo D'Areia, Cachoeira do Sul, 96503-205, Rio Grande do Sul, Brazil
robertrafaelvg@gmail.com, maikson.tonatto@ufsm.br
[2]Laboratory of Agroindustrial Processes Engineering (LAPE), Federal University of Santa Maria (UFSM)
1040, Sete de Setembro St., Downtown, Cachoeira do Sul, 96508-010, Rio Grande do Sul, Brazil
giovani.zabot@ufsm.br

Abstract. The Brazilian Space Program has advanced in the development and production of microsatellite launch vehicle (MLV) aiming at having self-sufficiency in sending satellites into space. Even though, the scientific literature is scarce of works that present detailed results on this type of launcher vehicle. Therefore, this work presents a structural analysis of a microsatellite launcher vehicle fairing manufactured by composite using a finite element (FE) model. The FE model was submitted to external pressure obtained from two-dimensional fluid dynamics simulations. A linear buckling simulation was performed to obtain the collapse pressure of the fairing and to determine the thickness of the composite laminates. Then, a non-linear static simulation was performed to obtain the progressive failure of the laminates using Hashin's criterion. Tree different stacking sequence were analyzed: $[\pm 28 / 0 / 0]_s$, $[90 / \pm 55_4 / 90]$ and $[\pm 65_5]$. The failure to the structure was obtained by mapping the pressure curve with the estimated thicknesses. Regarding the results, it was seen that the first buckling mode occurs before the material failure in all the stacking sequence conditions.

Keywords: Composites, Fairing, Finite element method, MLV, Structural analysis.

1 Introduction

With the development of sounding rockets, the Brazilian Space Program guaranteed autonomy and a technological base to proceed with projects aimed at launcher vehicles. Among them, the satellite launch vehicle (SLV) or in Brazil as VLS-1 was created, which suffered a break due to technical problems. The microsatellite launch vehicle (MLV) or in Brazil as VLM-1 is a new technology, which is a suborbital controlled vehicle with three stages. It is simpler than VLS-1, having a versatile configuration and with the purpose to launcher microsatellites in low equatorial orbit or reentry [1, 2].

There are few studies in the scientific literature aimed specifically at the structural analysis of the VLM-1. However, a range of works is seen, which focuses on the use of composites in aircraft and the distribution of aerodynamic loads in Brazilian launcher vehicles. Ribeiro et al. [3] performed numerical simulations to ensure structural and aerodynamic reliability for greater precision in the parameters of the RD-08 rocket. Ahamed [4] made a comparison between some materials commonly used in rocket structures, such as aluminum, carbon fiber/epoxy composite and metals. Lesage et al. [5] developed a new design of rocket structure made from carbon fiber–reinforced polymer (CFRP) and glass fiber–reinforced polymer (GFRP). The compressive loads, buckling limits, and bending moments in flight were evaluate. Leal [6] carried out a numerical study to analyze the aerodynamics of the VLM-1.

Based on this context, this work aims carry out a numerical calculation methodology for the design of a MLV to predict the structural behavior fairing using the finite element (FE) model. Two models were carry out, one is a linear buckling simulation to obtain the collapse pressure of the fairing and other a non-linear static simulation to

obtain the progressive failure of the laminates using Hashin criterion. Different stacking sequence of laminate used in fairing were evaluate and analyzed their potentialities and limitations.

2 Methodology

2.1 Geometry and constitutive laws

The developed geometry used in this study is based on the technical drawings of the model for the VLM-1 created by Mata [7]. The launcher vehicle have a height of 18.025 m and a diameter of 1.46 m in real scale, as represented in Fig. 1. The fairing was made using carbon fiber laminates. An external ply of aluminum is used as hubcap applied to the nose cone and, over the aluminum ply, has been added one glass fiber lamina.

The carbon fiber laminates were evaluated with three different stacking sequences in order to verify the effects of the composite layers on the structural behavior of the fairing. The stacking sequences of the carbon fiber/epoxy laminates $[\pm 28 / 0 / 0]_s$, $[90 / \pm 55_4 / 90]$ and $[\pm 65_5]$ were used. According to Cai [8], Almeida [9], and Lesage et al. [5], such configurations presented high strength when the cylinders were subjected to external and internal pressure. The stacking sequence values represent the angle β of inclination of the fiber in each layer. All configurations were based on the axial axis in the cylindrical geometry coordinate system for the longitudinal distance of the fiber. The angles were projected starting from the axial axis of the geometry as shown in Fig. 1, where f is the longitudinal axis of the fiber and β is the angle of inclination of the fiber.

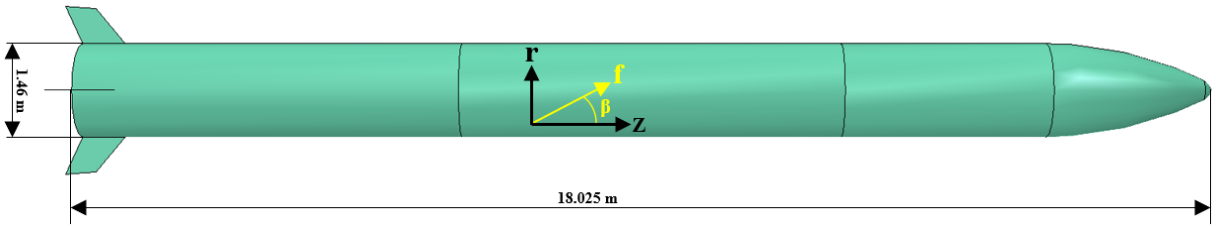

Figure 1. Geometry of the vehicle and fiber angle orientation in the Z-r plane

Table 1 shows the mechanical properties of carbon fiber/epoxy laminate, T800S/Epoxy 8551-7, and glass fiber/epoxy, Glass-S2/Epoxy, which were obtained from MECH software - Gcomp [10] and TORAY company datasheet [11]. Besides, the aluminum 7050-T7651 was used as an elastoplastic model, with a elasticity modulus equal to 71,700 MPa and a Poisson's ratio equal to 0.33 until yields stress [12].

Table 1. Mechanical properties of composite laminates

	T800S/Epoxy 8551-7	Glass-S2/Epoxy
E_1 (Mpa)	163500	55847
E_2 (Mpa)	8915	17926
ν_{12}	0.306	0.27
G_{12} (Mpa)	2925	6205
G_{13} (Mpa)	2925	6205
G_{23} (Mpa)	2441	3891
σ_1^T (Mpa)	3234	2000
σ_1^C (Mpa)	1932	965
σ_2^T (Mpa)	85	62
σ_2^C (Mpa)	112	155
τ_{12} (Mpa)	92	93
τ_{13} (Mpa)	92	93
G_{ftc} (kJ/m^2)	105	95
G_{fcc} (kJ/m^2)	108	103
G_{mtc} (kJ/m^2)	0.2	0.2
G_{mcc} (kJ/m^2)	0.2	0.2

Where, E_1 is the longitudinal elasticity modulus; E_2 and E_3 are the transverse elasticity modulus; ν_{12} is the in plane Poisson's ratio; G_{12}, G_{13} and G_{23} are in planes 1-2, 1-3 and 2-3 shear modulus, respectively; σ_1^T is the longitudinal tensile strength, σ_1^C is the longitudinal compressive strength, σ_2^T is the transverse tensile strength, σ_2^C is the transverse compressive strength, τ_{12} is the in plane shear strength and τ_{13} is the out-of-plane shear strength; G_{fcc}, G_{ftc}, G_{mtc} and G_{mcc} are the fracture energies.

2.2 FE model: Buckling and failure analyses

Figure 2 shows the finite element model developed from the MLV fairing. Mechanical properties were assigned separately in the regions, where carbon fiber/epoxy laminate was applied over the entire surface of the vehicle and the nose cone received an additional outer layer of aluminum and glass fiber/epoxy laminate. An angle of 0º was used for layer of glass fiber/epoxy composite for condition $[\pm 28 / 0 / 0]_s$, while for the conditions $[90 / \pm 55_4 / 90]$ and $[\pm 65_5]$, an angle of 90° was used. Regarding the fiber orientation, local coordinate systems were generated with dispositions based on the surface of the geometry as shown in the details of Fig. 2. Each layer has three integration points, making it possible to calculate the stresses in bottom, middle and top regions of layer.

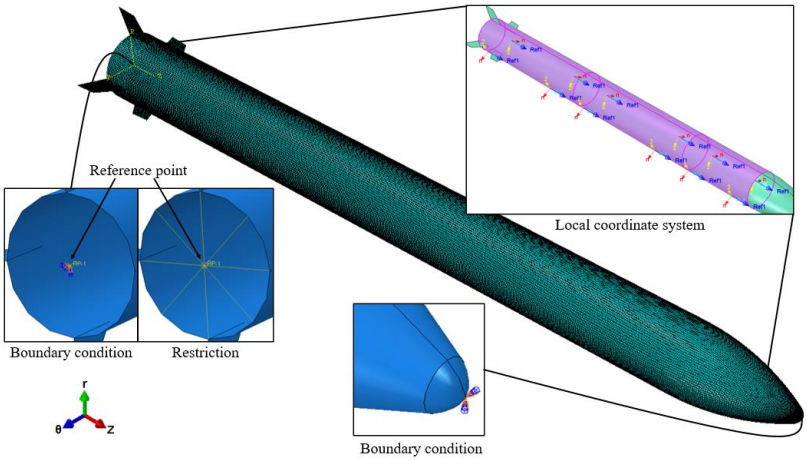

Figure 2. Finite element model of the MLV fairing

Regarding the bucking analysis, simulations were carried out using uniform external pressure along the structure. The effect of the thickness on collapse pressure of the structure was evaluate. The thickness was modified in order to obtain a collapse pressure higher than the maximum absolute pressure of 75 kPa obtained in the critical operating pressure. The thickness varied from 4 mm to 11.2 mm for the entire laminate during the analysis. The internal laminates were included in order to divide the stages with a sufficient thickness to guarantee that the buckling occurs in external surface of fairing and the fin module was disregarded.

In order to apply the boundary conditions, it was necessary to create some constraints. In the center of the base of the structure, a reference point (RP) was used as a control point for the base circumference, where the six degrees of freedom were restricted and with a kinematic-type coupling between the RP and the circumference edge. Furthermore, two boundary conditions were applied, the first being located in the RP, where all translations and rotations were fixed, and in the opposite point free axial rotation and displacement was allowed. The external pressure was fully applied to the entire external surface of the vehicle fairing. The generated mesh was linear with a total 22164 elements, which were characterized as S4R-type shell elements. Then, a buckle-type step was created to simulate linear buckling with the subspace solution system with five requested eigenvalues, one hundred vectors used per iteration and with a maximum of thirty iterations acting with incremental simulations.

The best condition obtained in the bucking analysis was used to evaluate the failure analysis of composite structure. The same boundary conditions of bucking analysis were used. The failure analysis was performed in order to identify what failure occurs first, bucking or failure caused by strength of composite laminates. The absolute pressure data was variable along of fairing. Then, the variable external pressure along of axial direction of fairing was applied. This variable external pressure was obtained from literature [6]. A nonlinear static type step

was created to establish the geometric and material nonlinearities, where an initial and maximum increment of 10% of total strength and a minimum increment of 0.001% were used. Comparison between results obtained with different mesh refinements was important due to the high dependence on the mesh on computational simulation solutions and the high sensitivity of failure in relation to the level of mesh refinement. The convergence study consisted of changing the global size of the elements, where the radial displacement along the vehicle fairing was the component used for comparison, ranging from 5131 to 400,784 elements.

3 Results and discussions

3.1 Effect of the number of mesh elements

Figure 3(a-b) shows the mesh convergence study obtained in FE model used for failure analysis. The mesh convergence study was performed in two points of interest in the vehicle fairing. A node located at the top of the second stage and another at the first point where the first stage joins the fins. The objective was to have a point that returned a maximum value of displacement or close to it. The radial displacements U2 and U3 were used to evaluate the mesh convergence. The red dashed lines indicate the values of 99.7% and 99.9% for U2 and U3, respectively, of the calculated displacement for the mesh with 400784 elements. The mesh convergence has occurred for meshes above of 89087 elements, considering the difference in displacement in relation to the more refined mesh. Therefore, the 89087 mesh elements value was chosen as the ideal one because it presented a good balance between computational cost and accuracy.

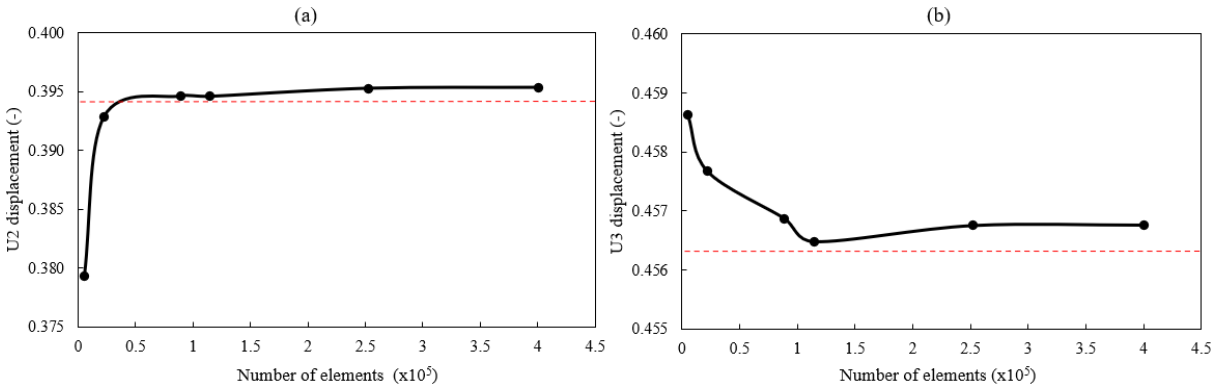

Figure 3. Graphs of (a) U2 and (b) U3 displacements versus number of elements

3.2 Effect of the thickness on buckling behavior

Figure 4 shows the collapse pressure vs. total thickness of composite laminates obtained in bucking analysis for three stacking sequence conditions. The collapse pressure corresponds to the eigenvalue of the 1st buckling mode, shows in Fig. 4. The 1st bucking mode presents larger regions of well-defined displacements in the three stages, where the central stage as the highest displacement. The red dashed line represents the maximum absolute pressure. According the curves, the collapse pressure increases faster in the stacking sequence $[90 / \pm 55_4 / 90]$ when the thickness was increase. Similar behavior was observed in $[\pm 65_5]$ condition, with a lower pressure. The stacking sequence $[\pm 28 / 0 / 0]_s$ presented lower collapse pressure when compared between all conditions. Above the red dashed line, it is seen the first pressure point where thicknesses of 10.4 mm were established for configuration $[\pm 28 / 0 / 0]_s$, 7 mm for configuration $[90 / \pm 55_4 / 90]$ and 7.2 mm for configuration $[\pm 65_5]$.

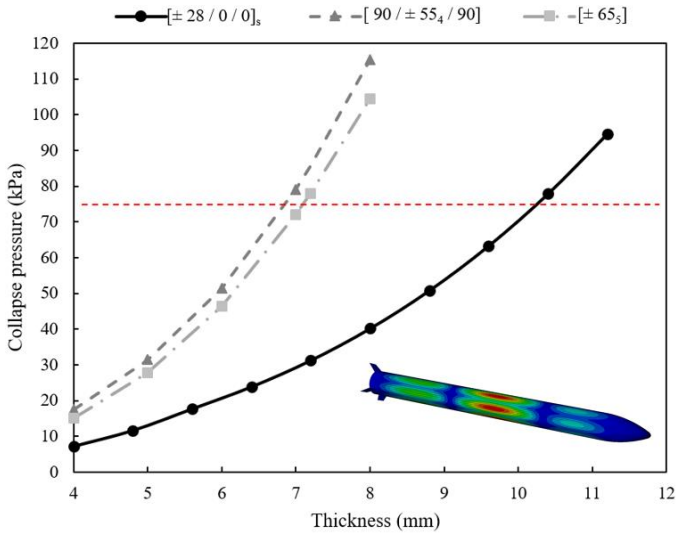

Figure 4. Collapse pressure versus total thickness of composite laminate curves

3.3 Effect of stacking sequence on failure analysis

Figure 5 depicts the Hashin's failure index for the stacking sequence of [± 65_5] with thickness of 7.2 mm. It is observed that the matrix compression index (Fig. 5b) presents maximum values between all index analyzed, with value ≈9.1×10^{-3} closed of the divisions between stages. The nose cone region presents index value of ≈6.1×10^{-3}. For fiber compression index (Fig. 5a), a maximum value of ≈1.3×10^{-5} was observed. Maximum values were observed in division between the stages nose cone region. For fiber tensile failure index (Fig. 5c) and matrix tensile index (Fig. 5d) present maximum values of ≈1.2×10^{-4} and ≈4.2×10^{-6}, respectively.

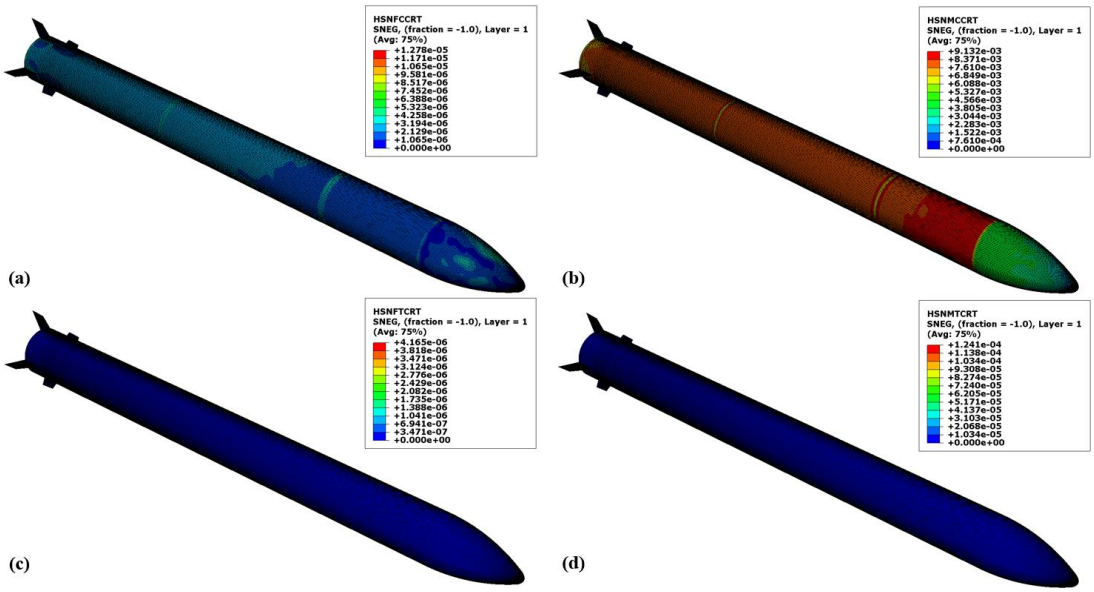

Figure 5. Hashin's failure index of stacking sequence of [± 65_5]: (a) fiber compression, (b) matrix compression, (c) fiber tension and (d) matrix tension.

Similar results were found to stacking sequence of [± 28 / 0 / 0]$_s$ and [90 / ± 55_4 / 90]. The differences in maximum values of [± 65_5] condition were 25.9% and 33.1% when compared with the conditions [± 28 / 0 / 0]$_s$ and [90 / ± 55_4 / 90], respectively. In fiber compression index, which was the second most relevant parameter, the condition [± 28 / 0 / 0]$_s$ had the highest index with maximum difference of 16.6% and 43.9% when compared to [90 / ± 55_4 / 90] and [± 65_5], respectively. In matrix traction index, the condition [± 65_5] had the highest value,

with difference of 75.8% and 58.7% when compared of $[\pm 28 / 0 / 0]_s$ and $[90 / \pm 55_4 / 90]$, respectively. In fiber tensile index, the model $[\pm 65_5]$ also had the highest value, with difference of 96.7% and 33% when compared with $[\pm 28 / 0 / 0]_s$ and $[90 / \pm 55_4 / 90]$, respectively.

Overall, all indices exhibit the highest values by matrix compression, with the highest one being very close to 1% in relation to the index equal to 1, referring to the conditions $[\pm 65_5]$. Therefore, no failures caused by strength limits of the composite material were observed in the failing. Then, the fairing structure does not show material damage in the three stacking sequences under the application of this pressure. Thus, among the configurations analyzed, the fairing when subjected to extreme pressures must first fail due to collapse (buckling).

4 Conclusions

The main objective of developing a methodology for calculating the mechanical behavior of the MLV fairing using numerical methods was achieved. Therefore, a sequence of activities on the analysis of the launcher vehicle fairing with the creation of geometry was reached. Also, material definition and stacking sequences followed by the development of a buckling evaluation to determine the collapse pressure and thickness of the fairing are obtained. Consequently, it was possible evaluate the structured failure index in a way compatible with the MLV. Thus, the stacking sequence $[90 / \pm 55_4 / 90]$ had the highest pressure to present buckling between configurations, requiring smaller material thicknesses for the external pressure imposed. The stacking sequence $[\pm 65_5]$ had a similar collapse pressure of the $[90 / \pm 55_4 / 90]$ with a maximum difference of 24.3% for thickness 10 mm. All indexes exhibit very low values, where matrix compression failure had the highest value for stacking sequence $[\pm 65_5]$. Therefore, the failure of failing was predominantly caused by bucking when the composite structure was subjected to external pressure.

Authorship statement. The authors hereby confirm that they are the sole liable persons responsible for the authorship of this work, and that all material that has been herein included as part of the present paper is either the property (and authorship) of the authors, or has the permission of the owners to be included here.

References

[1] ___. VLS-1. 2019. Available at: <http://www.iae.cta.br/index.php/todos-os-projetos/todos-os-projetos-desenvolvidos/projetos-vls1>. Accessed on: Mar 5th, 2020.
[2] ___. VLM-1. 2020. Available at: <http://www.iae.cta.br/index.php/todos-os-projetos/projetos-aeronautica/projetos-vlm-1>. Accessed on: Mar 5th, 2020.
[3] R. G. B. Ribeiro, A. D. Bahdur, N. S. Miquelin, J. P. T. Ribeiro, G. A. H. C. C. Lima and V. N. Capacia. ITA Rocket Design's eighth student built rocket, codenamed RD – 08. Project technical report, Spaceport America Cup, 2018.
[4] S. N. Ahamed et al., "Modeling And Analysis Of Rocket Outer Shell". *International Journal of Scientific & Technology Research*, v. 3, n. 4, p. 270–280, 2014.
[5] J. Lesage, S. Papais, C. Cossette, L. Dam-Quang, D. Lisus, K. Kolosova and J. Otis-Laperrire. McGill Rocket Team Project Blanche. Project technical report, Spaceport America Cup, 2018.
[6] F. H. Leal. Estudo numérico de cargas aerodinâmicas em foguete. Undergraduate thesis, University of Brasília, 2017.
[7] H. O. DA Mata. Procedimento Experimental para Análise Aerodinâmica do Veículo Lançador de Microssatélites VLM-1. Undergraduate thesis, Technological Institute of Aeronautics, 2013.
[8] B. Cai, Y. Liu, Z. Liu, X. Tian, R. Ji and Y, Zhang, "Probabilistic analysis of composite pressure vessel for subsea blowout preventers". *Engineering Failure Analysis*, v. 19, p. 97–108, 2012.
[9] J. H. S. Almeida, M. L. Ribeiro, V. Tita and S. C. Amico, "Damage and failure in carbon/epoxy filament wound composite tubes under external pressure: Experimental and numerical approaches". *Materials & Design*, v. 96, p. 431–438, 2016.
[10] ___. Software MECH-Gcomp. 2021. Available at: <https://gcomp-srv01.nuvem.ufrgs.br>. Accessed on: Mar 12th, 2021.
[11] ___. T800S Intermediate Modulus Carbon Fiber. Datasheet, rev. 1, Toray Composite Materials America, 2018.